Over 6% Efficient $Cu(In,Ga)Se_2$ Solar Cell Screen-Printed from Oxides on FTO

Viviana Sousa,[a] *Bruna F. Gonçalves,*[a,b] *Yitzchak S. Rosen,*[c] *José Virtuoso,*[a] *Pedro Anacleto*[a], *M. Fátima Cerqueira,*[a,b] *Evgeny Modin,*[d] *Pedro Alpuim,*[a,b] *Oleg I. Lebedev,*[e] *Shlomo Magdassi,*[c] *Sascha Sadewasser,*[a] *and Yury V. Kolen'ko*[*,a]

[a] International Iberian Nanotechnology Laboratory, Braga 4715-330, Portugal

[b] Center of Physics, University of Minho, Braga 4710-057, Portugal

[c] Casali Center of Applied Chemistry, Institute of Chemistry, The Hebrew University of Jerusalem, Jerusalem 91904, Israel

[d] CIC nanoGUNE, Donostia, San Sebastian, Spain

[e] Laboratoire CRISMAT, UMR 6508, CNRS-ENSICAEN, Caen 14050, France

AUTHOR INFORMATION

Corresponding Author

*yury.kolenko@inl.int

ABSTRACT.

A new approach to fabricate $Cu(In,Ga)Se_2$ solar cells on FTO is reported, where commercial CuO, In_2O_3 and Ga_2O_3 are formulated into high-quality ink based on ethyl cellulose solution in terpineol. From this ink, a 2 μm photoabsorber layer is fabricated by robust screen printing followed by thermal selenization, during which the final $Cu(In,Ga)Se_2$ is formed via chemical conversion of the pristine oxides into ternary selenide. The high homogeneity and good adhesion properties of the oxides' ink play an important role in obtaining dense and highly crystalline photoabsorber layers. The subsequent deposition of the n-type CdS buffer layer (heterojunction), the resistive i-ZnO layer, and the ZnO:Al transparent conducting window leads to a reliable photovoltaic device with an efficiency over six per cent. This finding reveals that solution-based screen printing from readily available oxide precursors provides an interesting cost-effective alternative to current vacuum- and energy-demanding processes of the $Cu(In,Ga)Se_2$ solar cell fabrication.

TOC GRAPHICS

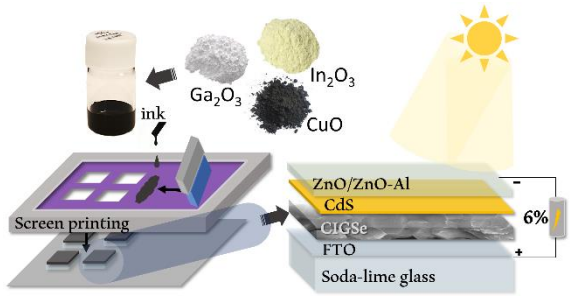

Solar cells are one of the most widely spread zero-emission energy generation technologies, which nowadays strongly rely on the first-generation silicon photovoltaics (PVs). Si PVs is, however, somewhat hampered by the significant energy demand required to produce about 100 μm-thick layer of high-purity silicon.[1–3] An interesting alternative to silicon PV is offered by second generation thin-film PVs based on $Cu(In,Ga)Se_2$ (CIGSe) material with chalcopyrite structure, and the champion power conversion efficiencies for CIGSe solar cells have recently reached 22.9%.[4] CIGSe is a direct band gap p-type semiconductor with high optical absorption coefficient, which advantageously allows to decrease the thickness of the photoabsorber layer of the respective solar cell down to a few μm (theoretically down to 0.5 μm, in reality down to 1–2 μm).[1] Additionally, the resultant CIGSe PV devices are very reliable, showing degradation of only ca. 0.5% per year.

Notably, the most efficient CIGSe PV devices are currently fabricated either by co-evaporation or by sputtering followed by a selenization step. Both are expensive fabrication techniques based on vacuum processing. Interestingly, industrially compatible solution-based coating technologies, such as screen printing, inkjet printing, spray coating, doctor blade coating, slot-die coating, or roll-to-roll processing, represent viable methods for reducing the energy demand of the CIGSe fabrication.[5] Motivated by the recent report of solution-processed $Cu(In,Ga)(S,Se)_2$ solar cells with 17.17% efficiency,[6] we became interested in developing a facile screen printing approach to CIGSe solar cells using commercially available CuO, In_2O_3 and Ga_2O_3 as the key constitute starting materials.

We selected screen printing because this deposition method is feasible for large scale production, and currently widely employed in textile industry. Specifically, screen printing technology consists of a screen with a pre-patterned mesh of appropriate size, wherein ink is forced

to pass through it with the help of a squeegee that forces the ink through the mesh in the direction of the substrate.[7] This technique produces μm-thick films, perfectly suiting the required thickness of CIGSe solar cells. By using appropriate mesh size while printing relatively viscous low volatile ink,[7] high-quality photoabsorber layers can be fabricated on large substrate area which is crucial for advancing printable CIGSe PV.

So far, most of the effort has focused on using inks based on $Cu(In,Ga)Se_2$ nanoparticles (NPs) or metallic precursors for solution-processed CIGSe solar cells, while only few reports are available for oxide-based inks.[8–12] Hence, we decided to leveraged on oxide precursors, since they are easy to synthetize, or even sometimes could be harvested directly from the earth crust,[10] and therefore are commercially readily available. In scarcity reports, where metal oxides were used as the precursors for screen printing ink formulation,[8–10] typically an intermediate thermal annealing step has to be used to reduce the pristine oxides into metals, followed by the selenization step to obtain the desired CIGSe phase. In this work, we present a robust and efficient screen printing approach towards CIGSe PV, which offers the practical advantage of avoiding the use of the reduction step. We also demonstrate the utility of this approach for the fabrication of CIGSe solar cells with the efficiency of over six per cent.

The initial point for our methodology was the formulation of high quality oxide-based ink for screen printing. For this purpose, we subjected the selected stoichiometric mixture of commercial Cu(II), In(III) and Ga(III) oxides to wet ball milling in the presence of di(propylene glycol) methyl ether and oleic acid. After this homogenization step, the resultant wet paste was dispersed in terpineol solvent containing ethyl cellulose to obtain viscous ink of the oxides. The ink was optimized to obtain a good stability, dispersion, wettability, and uniformity of the screen-printed pattern on the substrate, as shown in Figure S1 in the Supporting Information (SI). After

successful screen printing of the as-formulated oxide ink on conductive fluorine-doped tin oxide (FTO) substrate, the obtained film was calcined at 400ºC to remove carbon-based residues, and subjected to the rapid selenization at 550ºC under 5%H_2/Ar flow. A detailed description of the ink formulation, screen-printing, calcination, and selenization is presented in the SI.

We first investigated the phase composition of the resultant film by powder X-ray diffraction (XRD). According to the XRD, the as-obtained sample is a phase mixture of FTO substrate and tetragonal Cu(In,Ga)Se_2 with the chalcopyrite structure (Figure 1a).[9,13,14] Furthermore, the phase analysis demonstrates no evidence of oxides or other phases being present in the sample, suggesting that the metal oxides react with selenium vapor under diluted hydrogen atmosphere, leading to the formation of the copper indium gallium diselenide, $2CuO + In_2O_3 + Ga_2O_3 + 4Se + 8H_2 = 2Cu(In,Ga)Se_2 + 8H_2O$. The convenience of this synthetic protocol is that the conversion of the oxides into crystalline CIGSe is accomplished in a single step under reductive atmosphere of H_2.

We further analyzed the local structure of the as-fabricated film by Raman spectroscopy (Figure 1b), and the results are consistent with the XRD. A major sharp peak at 173 cm^{-1} with full width at half maximum (FWHM) of 11 cm^{-1} corresponds to the A_1 vibrational mode of CIGSe.[15,16] The broader peaks at 120 and 218 cm^{-1} are in good agreement with the B_1 and B_2/E modes of CIGSe, respectively.[16,17] Interestingly, we observed a shoulder peak at 188 cm^{-1}, which is not associated with any Cu–In–Ga–Se phases. Hence, the detected band is likely due to A_{1g} mode of $SnSe_2$ compound,[15] suggesting alloying of Sn from the FTO into the CIGSe layer (*see below*).

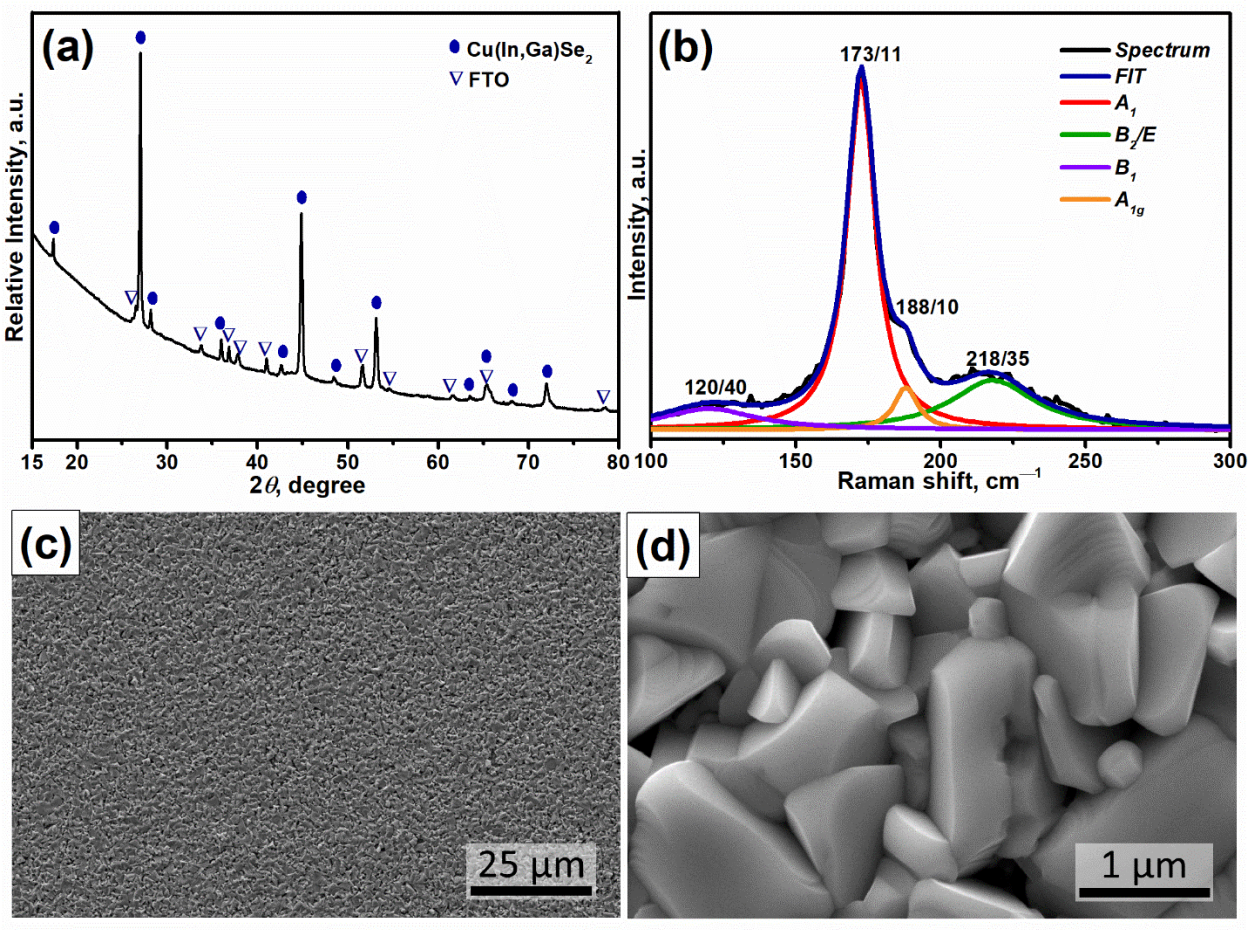

Figure 1. (a) XRD pattern of the CIGSe photoabsorber layer on FTO substrate. Ovals and triangles correspond to the positions of the most intense Bragg reflections expected for CIGSe (ICDD No. 01-083-3357, tetragonal, I–42d) and FTO, respectively. (b) Lorentzian fit (blue) to the experimental Raman data (black) for the CIGSe photoabsorber layer. The position/FWHM (in cm^{-1}) is provided for each component. Top surface low (c) and high (d) magnification SEM images of the as-fabricated CIGSe film.

We next studied the morphology, chemical composition and stoichiometry of the obtained CIGSe photoabsorber layer by means of scanning electron microscopy (SEM) in conjunction with energy dispersive X-ray spectroscopy (EDX). Figures 1c,d show the overall top-view morphology of the resultant photoabsorber deposited on FTO. CIGSe across the film exhibits a uniform and reasonably dense appearance of µm-sized crystals, indicating significant grain growth of the CIGSe phase during selenization. Accordingly, the surface of the photoabsorber layer is quite rough, which is a result of random orientation of the inter-grown CIGSe crystals. The EDX analyses show that the CIGSe phase is depleted in Ga and In in comparison to the initial oxides'

ratio Cu/(In+Ga) of 0.8 and Ga/(In+Ga) of 0.3, exhibiting after selenization the ratio Cu/(In+Ga) of 1.0 and Ga/(In+Ga) of 0.23.

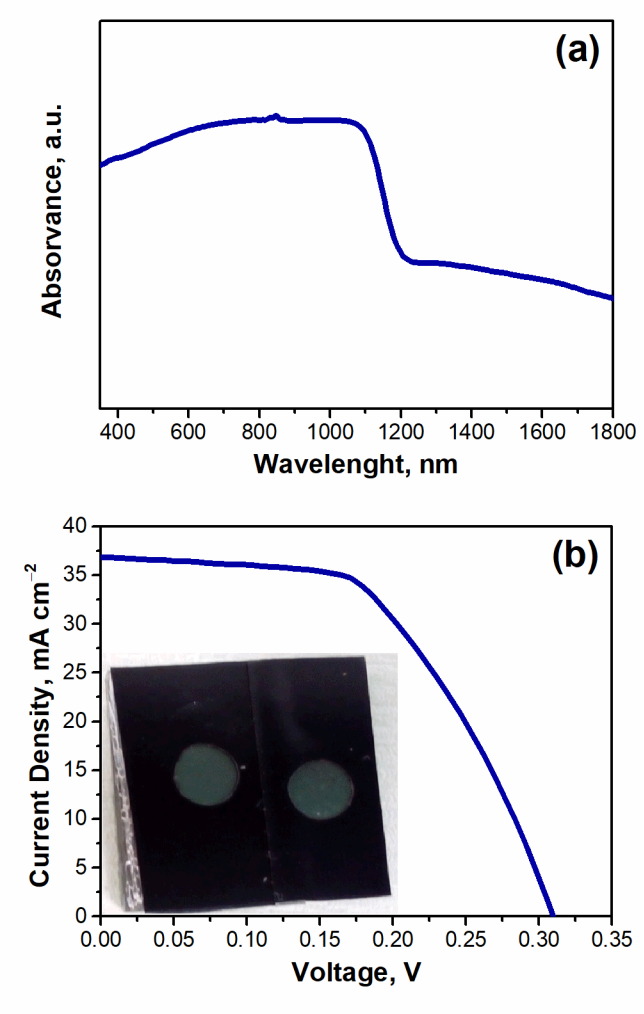

Figure 2. (a) UV–Vis–NIR absorption spectrum of a representative CIGSe film. (b) *I–V* curve of final PV device reaching 6.1% efficiency, J_{sc} of 36.8 mA/cm-^{2}, V_{oc} of 0.31 V and *FF* of 53.8% (inset picture of PV device).

Our CIGSe film, uniformly deposited over FTO via screen printing followed by selenization, was further evaluated in terms of optical properties using ultra-violet, visible and near infra-red spectroscopy (UV–Vis–NIR). The collected UV–Vis–NIR spectrum shows that the as-fabricated CIGSe film absorbs strongly through the visible and into the near-infrared region (Figure 2a). To calculate the direct bandgap (E_g), the following equation was used: $E_g = h \times c/\lambda$, where h is the Planck's constant, c is the speed of light and λ is the absorption cutoff wavelength

on the absorption edge, obtained from the absorption spectra.[18] The optical absorption edge of the resultant CIGSe layer was estimated to be 1.04 eV, which is slightly lower as compared with the optimal values (1.1–1.14 eV) reported previously for bulk CIGSe chalcopyrite.[2,5]

The characterization data above evidence that our screen printing of oxide-based ink followed by selenization allows access to semiconducting CIGSe photoabsorber layer. Accordingly, we moved forward with the fabrication of CIGSe solar cell devices, the details of the device fabrication are summarized in the SI. Briefly, to create a heterojunction, we first deposited 70-nm buffer layer of n-type CdS using chemical bath deposition on top of the freshly fabricated ≈2 μm-thick CIGSe film on FTO glass. Next, 50-nm resistive layer of intrinsic zinc oxide (i-ZnO) was sputtered on FTO/CIGSe/CdS, and finally the PV device was finished by sputtering 200-nm transparent conducting window of Al-doped zinc oxide (ZnO:Al). This fabrication procedure afforded reliable FTO/CIGSe/CdS/i-ZnO/ZnO:Al PV devices. The top morphology of the device is shown in Figure S2. One can see that although the overall surface of the PV device is reasonably rough due to the roughness of the original CIGSe layer (Figure 1c,d), the top window ZnO:Al and resistive i-ZnO layers were homogeneously deposited onto the surface of FTO/CIGSe/CdS.

We further conducted cross-sectional investigation of the resultant PV device. For this purpose, a focused ion beam (FIB) was employed for cross-sectioning of the film. The representative SEM images of the obtained lamella are shown in Figure S3, while Figure 3 summarizes the scanning transition electron microscopy (STEM) investigation of the lamella. A multilayered microstructure of the PV device is confirmed by SEM and STEM observations, albeit one can clearly see the existence of voids microstructural defects at the interface between FTO substrate and CIGSe layer (Figures S3, 3a), consistent with the literature.[19] The grains of photoabsorber CIGSe layer itself are highly crystalline and structural defects free, as one can see

from the representative high-angle annular dark-field (HAADF) STEM images and the corresponding selected area electron diffraction (SAED) patterns (Figures 3b–d). Regardless the aforementioned voids observed at the FTO/CIGSe interface, our HAADF–STEM imaging of the interface reveals nearly epitaxial growth of the CIGSe on top of FTO substrate (Figure 3e), suggesting the existence of reasonably good electrical contact between photoabsorber and back contact.

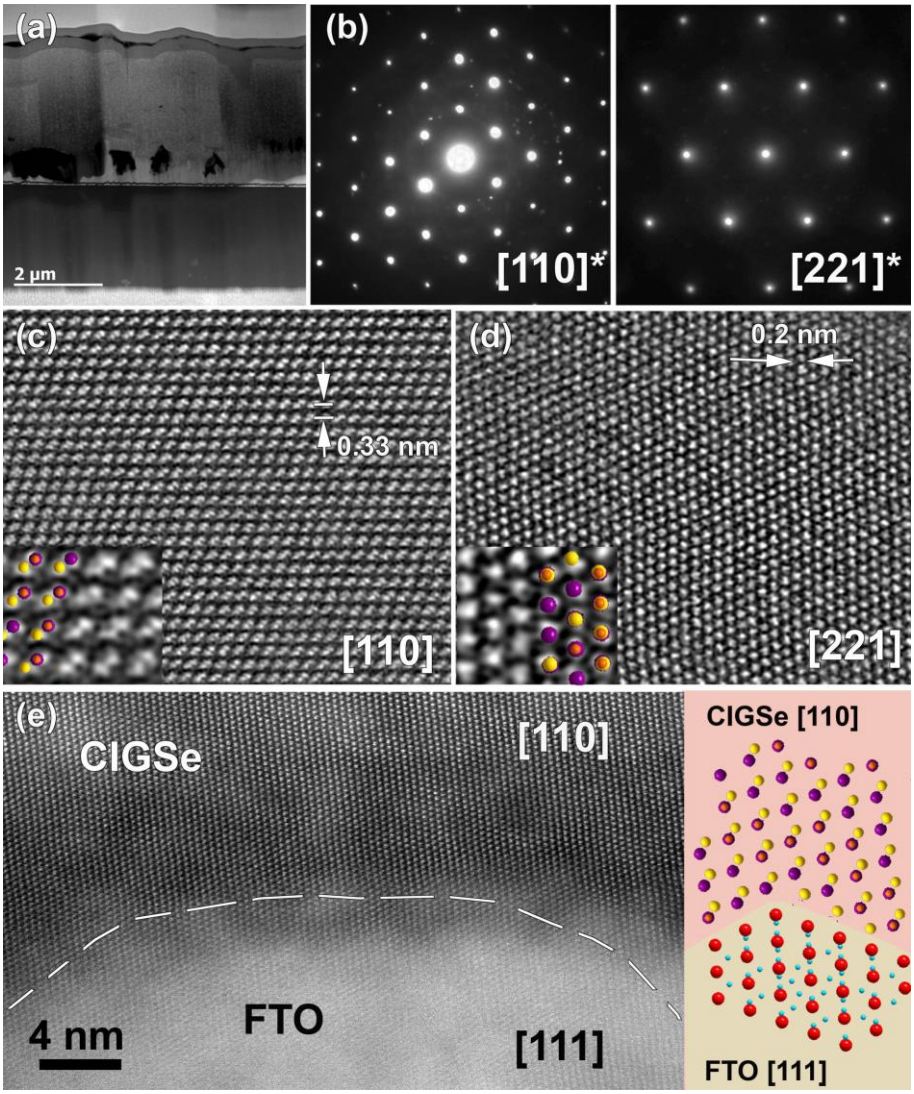

Figure 3. (a) Cross-sectional HAADF–STEM image of the fabricated FTO/CIGSe/CdS/i-ZnO/ZnO:Al PV device. (b) SAED patterns corresponding to the high-resolution HAADF-STEM images (c, d) of the CIGSe layer along [110] and [211] zone axes. (e) High-resolution HAADF-STEM image of the interface between FTO and CIGSe, demonstrating nearly epitaxial growth of [110] CIGSe on [111] FTO together with the corresponding structural model.

After fabrication and structural characterization of the PV device, we assessed the photovoltaic performance of the FTO/CIGSe/CdS/i-ZnO/ZnO:Al solar cell (Figure 2b). The solar cell exhibits a short-circuit current density (J_{sc}) of 36.8 mA cm^{-2}, open-circuit voltage (V_{oc}) of 0.31 V, and fill factor (FF) of 53.8%. These values lead to a 6.1% efficiency of the resultant solar cell. The high short-circuit current obtained can be correlated with low bandgap (1.04 eV) obtained for the CIGSe photoabsorber layer. As for the V_{oc}, a significantly reduced value was measured, which we attribute to recombination losses and to the low bandgap. Regarding the *FF* value, the associated series resistance is dominating *FF*, which could be related to interface problems between back contact and photoabsorber, such as presence of the voids.

To better understand fine aliment of solar cell layers, cross-sectional chemical composition of the PV device was analyzed by EDX in STEM mode. Figure 4 shows representative STEM−EDX mapping of the working FTO/CIGSe/CdS/i-ZnO/ZnO:Al PV device. Starting from top of the PV device, the presence of In is detected in CdS layer, resulting in CdS+In composition of the resultant buffer layer responsible for heterojunction. Furthermore, the distribution of Ga within the CIGSe layer was found to be markedly inhomogeneous, showing the existence of segregated Ga–O phases within the photoabsorber layer, which is more clearly detailed in Figure S4. Notably, we were using commercial CuO and In_2O_3 nanopowders for ink formulation, while Ga_2O_3 nanopowder commercially is not available, and therefore, we were using polycrystalline Ga_2O_3 as a precursor. It seems to be, that even after wet ball milling, the size of Ga_2O_3 is not reduced down to nanometer size, thus resulting in the existence of not fully reacted Ga–O phase in the CIGSe layer due to the low reactivity of the large particles. Accordingly, the lack of a sufficient amount of Ga in the CIGSe layer could contribute to its reduced band gap value and accordingly low V_{oc}.[20] In addition, the presence of the Ga–O phase inclusions in CIGSe layer can

be considered as recombination centers for holes and electrons, thus lowering the overall PV device performance.

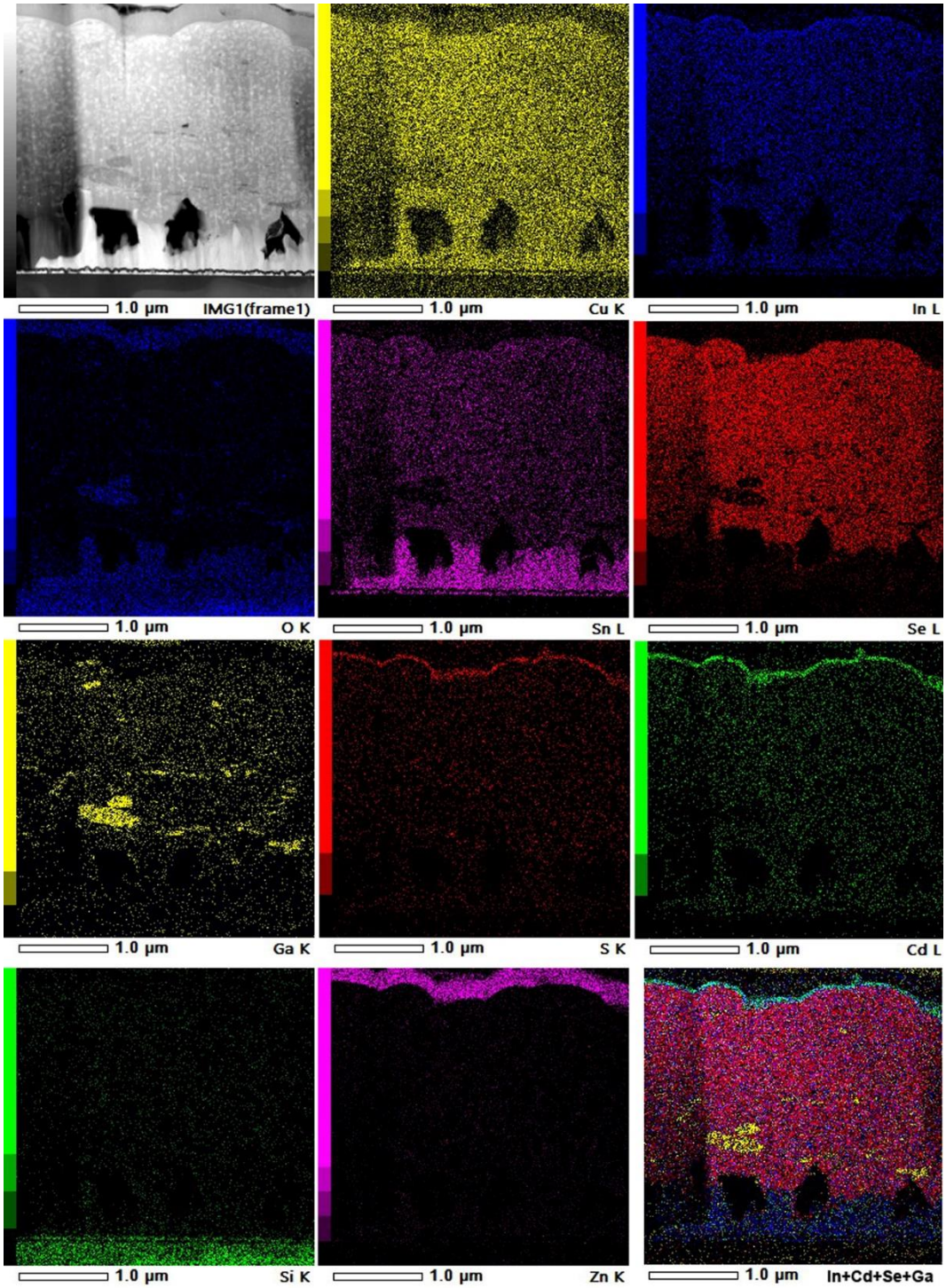

Figure 4. Cross-section HAADF−STEM image of the ZnO:Al/i-ZnO/CdS/CIGSe/FTO PV device, together with the simultaneously collected EDX maps of Cu, In, O, Sn, Se, Ga, S, Cd, Si, Zn, as well as In, Cd, Se, Ga mixture.

Interestingly, from Figure 4, the migration of tin from FTO into CIGSe layer is clearly observed, resulting in an intermixing of Sn, Cu and In at the FTO/CIGSe interface. This migration most likely occurs during the selenization process and leads to formation of the aforementioned voids defects at the interface between photoabsorber and back contact.[19] Such modification of the FTO back contact possibly gives rise to rear interface recombination, hence, lowering V_{oc} and the final device performance.[10] The interface recombination also gives rise to moderate FF as a result of high series resistance, suggesting that further improvements of the absorber/back junction should be conducted to avoid recombination losses and associated high series resistance.[10,12,21,22]

Notably, soda–lime glass (SLG) with ≈0.5 μm layer of molybdenum is known to be a good substrate/back contact for CIGSe solar cells, and we initially employed this Mo/SLG type of substrate in our screen-printing-assisted fabrication procedure. Unfortunately, we experimentally found that Mo cannot resist selenization at 550ºC for 30 min under 5%H_2/Ar flow, entirely transforming into $MoSe_2$ (confirmed by XRD). This transformation resulted in the strong peeling of the resultant CIGSe layer from the SLG substrate (Figure S5). Importantly, by switching the back contact to FTO, we demonstrated that reliable CIGSe solar cell can be fabricated.

In conclusion, we describe a robust printing-based method for the fabrication of CIGSe solar cells. Oxide ink formulation, screen-printing, and calcination followed by selenization provide ≈2 μm thick crystalline CIGSe photoabsorber layers grown on top of FTO/glass substrates. One of the key points of this route is that the oxides' reduction and selenization are conducted in a single step. After completing the photoabsorber layer with the buffer and window layers, the final FTO/CIGSe/CdS/i-ZnO/ZnO:Al solar cell device exhibited 6.1% efficiency. To the best of our knowledge, this is the topmost performance for CIGSe solar cell fabricated from oxide precursors on FTO (Table S1).[4-6,8/10/12/18/23-32] We believe that the demonstrated feasibility of our

screen printing approach from oxides can inspire new research efforts for fabricating fully printed CIGSe PV in a cost-effective manner.

Our investigation further showed that the PV properties are strongly influenced by interface recombination due to compositional and microstructural variation within PV device, suggesting that improvements should be done to enhance the device performance by optimizing the photoabsorber/back contact interface and the chemical composition of the CIGSe phase. This is the subject of our ongoing research.

ASSOCIATED CONTENT

The supporting information (SI) is available free of charge on the ACS Publications website. Materials and methods and additional optical microscopy, electron microscopy and visualization data (PDF).

CORRESPONDING AUTHOR

*yury.kolenko@inl.int

Notes

The authors declare no competing financial interest.

ACKNOWLEDGEMENT

We thank all members of the Nanochemistry Research Group at INL for valuable discussions. This work was supported by ERDF COMPETE 2020 and Portuguese FCT funds

under the PrintPV project (PTDC/CTM-ENE/5387/2014, Grant Agreement No. 016663). B.F.G. is grateful to the FCT for the SFRH/BD/121780/2016 grant.

REFERENCES

(1) Coughlan, C.; Ibáñez, M.; Dobrozhan, O.; Singh, A.; Cabot, A.; Ryan, K. M. Compound Copper Chalcogenide Nanocrystals. *Chem. Rev.* **2017**, *117*, 5865–6109.

(2) Ramanujam, J.; Singh, U. P. Copper Indium Gallium Selenide Based Solar Cells – a Review. *Energy Environ. Sci.* **2017**, *10*, 1306–1319.

(3) Terheiden, B.; Ballmann, Tabitha Horbelt, R.; Schiele, Y.; Seren, S.; Ebser, J.; Hahn, G.; Mertens, V.; Koentopp, M. B.; Scherff, Maximilian Müller, J. W.; Holman, Zachary C. Descoeudres, A.; et al. Manufacturing 100-µm-Thick Silicon Solar Cells with Efficiencies Greater than 20% in a Pilot Production Line. *Physica Status Solidi A*. 2014, pp 1–12.

(4) Kato, T.; Wu, J.; Hirai, Y.; Sugimoto, H.; Bermudez, V. Record Efficiency for Thin-Film Polycrystalline Solar Cells Up to 22.9% Achieved by Cs-Treated Cu(In,Ga)(Se,S)$_2$. *IEEE J. Photovoltaics* **2018**, *9*, 325–330.

(5) Roux, F.; Amtablian, S.; Anton, M.; Besnard, G.; Bilhaut, L.; Bommersbach, P.; Braillon, J.; Cayron, C.; Disdier, A.; Fournier, H.; et al. Chalcopyrite Thin-Film Solar Cells by Industry-Compatible Ink-Based Process. *Sol. Energy Mater. Sol. Cells* **2013**, *115*, 86–92.

(6) Eeles, A.; Arnou, P.; Bowers, J. W.; Walls, J. M.; Whitelegg, S.; Kirkham, P.; Allen, C.; Stubbs, S.; Liu, Z.; Masala, O.; et al. High-Efficiency Nanoparticle Solution-Processed Cu(In,Ga)(S,Se)$_2$ Solar Cells. *IEEE J. Photovoltaics* **2018**, *8*, 288–292.

(7) Krebs, F. C. Fabrication and Processing of Polymer Solar Cells: A Review of Printing and

Coating Techniques. *Sol. Energy Mater. Sol. Cells* **2009**, *93*, 394–412.

(8) Kapur, V. K.; Bansal, A.; Le, P.; Asensio, O. I. Non-Vacuum Processing of $CuIn_{1-x}Ga_xSe_2$ Solar Cells on Rigid and Flexible Substrates Using Nanoparticle Precursor Inks. *Thin Solid Films* **2003**, *431–432*, 53–57.

(9) Lee, E.; Park, S. J.; Cho, J. W.; Gwak, J.; Oh, M. K.; Min, B. K. Nearly Carbon-Free Printable CIGS Thin Films for Solar Cell Applications. *Sol. Energy Mater. Sol. Cells* **2011**, *95*, 2928–2932.

(10) Pulgarín-Agudelo, F. A.; López-Marino, S.; Fairbrother, A.; Placidi, M.; Izquierdo-Roca, V.; Sebastián, P. J.; Ramos, F.; Pina, B.; Pérez-Rodríguez, A.; Saucedo, E. A Thermal Route to Synthesize Photovoltaic Grade $CuInSe_2$ Films from Printed CuO/In_2O_3 Nanoparticle-Based Inks under Se Atmosphere. *J. Renew. Sustain. Energy* **2013**, *5*, 053140.

(11) Kuo, H. P.; Tsai, H. A.; Huang, A. N.; Pan, W. C. CIGS Absorber Preparation by Non-Vacuum Particle-Based Screen Printing and RTA Densification. *Appl. Energy* **2016**, *164*, 1003–1011.

(12) López-García, J.; Xie, H.; Izquierdo-Roca, V.; Sylla, D.; Fontané, X.; Blanes-Guardia, M.; Ramos, F.; Espindola-Rodriguez, M.; López-Marino, S.; Saucedo, E.; et al. Synthesis of $CuIn(S,Se)_2$ Quaternary Alloys by Screen Printing and Selenization-Sulfurization Sequential Steps: Development of Composition Graded Absorbers for Low Cost Photovoltaic Devices. *Mater. Chem. Phys.* **2015**, *160*, 237–243.

(13) Zhang, C.; Zhu, H.; Liang, X.; Zhou, D.; Guo, Y.; Niu, X.; Li, Z.; Chen, J.; Mai, Y. Influence of Heating Temperature of Se Effusion Cell on $Cu(In,Ga)Se_2$ Thin Films and Solar Cells.

Vacuum **2017**, *141*, 89–96.

(14) Cheng, K.; Han, K.; Kuang, Z.; Jin, R.; Hu, J.; Guo, L.; Liu, Y.; Lu, Z.; Du, Z. Optimization of Post-Selenization Process of Co-Sputtered CuIn and CuGa Precursor for 11.19% Efficiency Cu(In,Ga)Se_2 Solar Cells. *J. Electron. Mater.* **2017**, *46*, 2512–2520.

(15) Yan, Y.; Guo, T.; Song, X.; Yu, Z.; Jiang, Y.; Xia, C. Cu(In,Ga)Se_2 Thin Films Annealed with $SnSe_2$ for Solar Cell Absorber Fabricated by Magnetron Sputtering. *Sol. Energy* **2017**, *155*, 601–607.

(16) Rincón, C.; Ramírez, F. J. Lattice Vibrations of $CuInSe_2$ and $CuGaSe_2$ by Raman Microspectrometry. *J. Appl. Phys.* **1992**, *72*, 4321–4324.

(17) Witte, W.; Kniese, R.; Powalla, M. Raman Investigations of Cu(In,Ga)Se_2 Thin Films with Various Copper Contents. *Thin Solid Films* **2008**, *517*, 867–869.

(18) Chen, Q.; Dou, X.; Li, Z.; Cheng, S.; Zhuang, S. Printed Ethyl Cellulose/$CuInSe_2$ Composite Light Absorber Layer and Its Photovoltaic Effect. *J. Phys. D. Appl. Phys.* **2011**, *44*, 455401.

(19) Jiang, J.; Yu, S.; Gong, Y.; Yan, W.; Zhang, R.; Liu, S.; Huang, W.; Xin, H. 10.3 % Efficient $CuIn(S,Se)_2$ Solar Cells from DMF Molecular Solution with the Absorber Selenized under High Argon Pressure. *Sol. RRL* **2018**, *1800044*, 1–7.

(20) Kim, B.; Min, B. K. Strategies toward Highly Efficient CIGSe Thin-Film Solar Cells Fabricated by Sequential Process. *Sustain. Energy Fuels* **2018**, *2*, 1671–1685.

(21) Nakane, A.; Tampo, H.; Tamakoshi, M.; Fujimoto, S.; Kim, K. M.; Kim, S.; Shibata, H.; Niki, S.; Fujiwara, H. Quantitative Determination of Optical and Recombination Losses in

Thin-Film Photovoltaic Devices Based on External Quantum Efficiency Analysis. *J. Appl. Phys.* **2016**, *120*, 064505.

(22) Cui, Y.; Zhang, Z.; Du, X.; Liu, W.; Liu, S.; Deng, Y.; Huang, X.; Wang, G. Efficient Hybrid Solution Strategy to Fabricate Cu(In,Ga)(S,Se)$_2$ Solar Cells. *J. Alloys Compd.* **2017**, *696*, 884–890.

(23) Zhao, Z.; Qi, Y.; Chen, Q.; Zheng, X.; Hao, Q.; Zhang, W.; Mao, J.; Liu, C.; Liu, H. Solution-Based Synthesis of Dense, Large Grained CuIn(S,Se)$_2$ Thin Films Using Elemental Precursor. *Ceram. Int.* **2017**, *43*, 6257–6262.

(24) Khavar, A. H. C.; Mahjoub, A. R.; Taghavinia, N. Low-Temperature Solution-Based Processing to 7.24% Efficient Superstrate $CuInS_2$ Solar Cells. *Sol. Energy* **2017**, *157*, 581–586.

(25) Mcleod, S. M.; Hages, C. J.; Carter, N. J.; Agrawal, R. Synthesis and Characterization of 15% Efficient CIGSSe Solar Cells from Nanoparticle Inks. *Prog. Photovoltaics Res. Appl.* **2015**, *23*, 1550–1556.

(26) Zhao, X.; Lu, M.; Koeper, M. J.; Agrawal, R. Solution-Processed Sulfur Depleted Cu(In, Ga)Se_2 Solar Cells Synthesized from a Monoamine–Dithiol Solvent Mixture. *J. Mater. Chem. A* **2016**, *4*, 7390–7397.

(27) Septina, W.; Kurihara, M.; Ikeda, S.; Nakajima, Y.; Hirano, T.; Kawasaki, Y.; Harada, T.; Matsumura, M. Cu(In,Ga)(S,Se)$_2$ Thin Film Solar Cell with 10.7% Conversion Efficiency Obtained by Selenization of the Na-Doped Spray-Pyrolyzed Sulfide Precursor Film. *ACS Appl. Mater. Interfaces* **2015**, *7*, 6472–6479.

(28) Uhl, A. R.; Katahara, J. K.; Hillhouse, H. W. Molecular-Ink Route to 13.0% Efficient Low-Bandgap $CuIn(S,Se)_2$ and 14.7% Efficient $Cu(In,Ga)(S,Se)_2$ Solar Cells. *Energy Environ. Sci.* **2016**, *9*, 130–134.

(29) Berner, U.; Colombara, D.; Wild, J. De; Robert, E. V. C.; Schütze, M.; Hergert, F.; Valle, N.; Widenmeyer, M.; Dale, P. J. 13.3% Efficient Solution Deposited $Cu(In,Ga)Se_2$ Solar Cells Processed with Different Sodium Salt Sources. *Prog. Photovoltaics Res. Appl.* **2016**, *24*, 749–759.

(30) Todorov, T. K.; Gunawan, O.; Gokmen, T.; Mitzi, D. B. Solution-Processed $Cu(In,Ga)(S,Se)_2$ Absorber Yielding a 15.2% Efficient Solar Cell. *Prog. Photovoltaics Res. Appl.* **2013**, *21*, 82–87.

(31) Arnou, P.; Cooper, C. S.; Uličná, S.; Abbas, A.; Eeles, A.; Wright, L. D.; Malkov, A. V.; Walls, J. M.; Bowers, J. W. Solution Processing of $CuIn(S,Se)_2$ and $Cu(In,Ga)(S,Se)_2$ Thin Film Solar Cells Using Metal Chalcogenide Precursors. *Thin Solid Films* **2017**, *633*, 76–80.

(32) Wu, S.; Jingjing, J.; Yu, S.; Gong, Y.; Yan, W.; Xin, H.; Huang, W. Over 12% Efficient Low-Bandgap $CuIn(S, Se)_2$ Solar Cells with the Absorber Processed from Aqueous Metal Complexes Solution in Air. *Nano Energy* **2019**, *62*, 818–822.